

Article

Ball Milled Gd Flakes Subjected to Heat Treatments: Structure, Magnetic and Magnetocaloric Properties

Andrey V. Svalov¹, Dmitriy S. Neznakhin¹, Andrey V. Arkhipov¹, Sergey V. Andreev¹, Nadezhda V. Selezneva¹, Aitor Larrañaga²  and Galina V. Kurlyandskaya^{1,3,*} 

¹ Institute of Natural Sciences and Mathematics, Ural Federal University, 620002 Ekaterinburg, Russia

² Advanced Research Facilities (SGIKER), Universidad del País Vasco UPV-EHU, 48080 Bilbao, Spain

³ Departamento de Electricidad y Electrónica, Universidad del País Vasco UPV/EHU, 48080 Bilbao, Spain

* Correspondence: kurlyandskaya.gv@ehu.es

Abstract: Gd flake samples were prepared by conventional ball milling technique starting from rapidly quenched Gd ribbons and followed by vacuum annealing in different conditions. Heat treatments were conducted in a vacuum at selected temperatures up to 600 K. The structural features, magnetic and magnetocaloric properties were comparatively analyzed. The change in magnetic entropy was calculated using an experimental set of magnetic isotherms measured in a wide range of temperatures. The variations in the refrigeration capacity and the exponent of the magnetic entropy change in the external magnetic field were carefully calculated and analyzed.

Keywords: crystal structure; entropy change; refrigeration capacity; ball milling; heat treatment



Citation: Svalov, A.V.; Neznakhin, D.S.; Arkhipov, A.V.; Andreev, S.V.; Selezneva, N.V.; Larrañaga, A.; Kurlyandskaya, G.V. Ball Milled Gd Flakes Subjected to Heat Treatments: Structure, Magnetic and Magnetocaloric Properties. *Magnetochemistry* **2022**, *8*, 138. <https://doi.org/10.3390/magnetochemistry8110138>

Academic Editor: Lotfi Bessais

Received: 22 September 2022

Accepted: 21 October 2022

Published: 23 October 2022

Publisher's Note: MDPI stays neutral with regard to jurisdictional claims in published maps and institutional affiliations.



Copyright: © 2022 by the authors. Licensee MDPI, Basel, Switzerland. This article is an open access article distributed under the terms and conditions of the Creative Commons Attribution (CC BY) license (<https://creativecommons.org/licenses/by/4.0/>).

1. Introduction

The special efforts of many researchers have recently been focused on the development of functional materials for the application of the magnetocaloric effect (MCE) in the field of eco-friendly magnetic refrigeration both near room temperature and for cryogenic applications [1–5]. A condition of the successful operation of a magnetic refrigerator is high efficiency in heat transfer between the working refrigerating body and the surroundings. The heat transfer can be facilitated by an increase in the surface-to-volume ratio for the working body. In addition to a high magnetocaloric effect, high thermal conductivity, appropriate mechanical properties for optimum design [6,7] and enhanced functionalities of the magnetocaloric devices are desired. The materials in the form of powder meet this requirement very well [8–11].

Now, due to a shortage of water and energy resources, physical and chemical techniques requiring a small amount of water and energy per unit of the obtained material are under special attention [12,13]. Ball milling is a well-known conventional technique for the fabrication of large, reproducible batches of different materials in a powder state down to nanosized powders [14–16]. Due to the milling process, in many cases, the reduction of the crystal size down to nanometric scales and the accumulation of defects in grain boundaries takes place [14]. For magnetic materials, this causes a decrease in the magnetization value and a slow change of magnetization near the phase transition temperature. Such changes lead to a decrease in the MCE effect value [7,8,11].

On the other hand, the magnetocaloric properties of powder samples can be enhanced through the nanostructuring of the initial material. Nanostructuring causes an increase in the Curie temperature distribution. In turn, it leads to a broadening of the peak of the temperature change of the magnetic entropy (ΔS_M) and an increase in a refrigeration capacity (RC) value. RC can be defined as the product of the maximum value of the peak of the magnetic entropy change and the width of ΔS_M peak at its half-height [1]. In addition, nanostructuring can enhance the field dependence of the magnetocaloric effect [11,14,17,18]. Moreover, appropriate annealing of polycrystalline materials can, to some extent, restore

the perfection of their crystal structure (due to the stress relaxation, movement of the vacancies, etc.) and magnetization behaviour.

In recent years, special progress has been made in the search for new magnetocaloric materials [1–3]. Nonetheless, gadolinium remains the most effective functional material for magnetic refrigerators operating both near room and at cryogenic temperatures [19]. Gadolinium is a well-studied collinear ferromagnet with a Curie temperature of $T_C = 294$ K [20]. Relatively recently, a formula accurately describing the spontaneous magnetization of M_s at an arbitrary temperature was proposed [21]. This made it possible to determine, with high accuracy, the exchange stiffness constant A , which is an important characteristic of ferromagnetic material [22]. At the same time, it is well known that severe plastic deformation of Gd reduces the magnetization to approximately one-half of that of polycrystalline Gd [23]. However, additional heat treatments of deformed Gd samples can establish an advantageous balance between the height and width of the magnetic entropy peak, which determines the RC value [23].

In this work, we presented the results of a detailed study of the influence of the heat treatment on the structure, magnetic and magnetocaloric properties of gadolinium powder obtained by the conventional ball milling technique starting from rapidly quenched Gd ribbons and followed by additional heat treatments.

2. Experiment

Bulk Gd has very good plasticity, and it is hard enough to be processed by mechanical crushing. Therefore, the well-known and highly productive conventional ball milling technique was used to obtain gadolinium powder for this study. Rapidly quenched gadolinium ribbons (3 mm wide and 70 μm thick [24]) were mechanically cut into small pieces a few mm long. These pieces of Gd ribbons were used as the primary material for the conventional ball milling fabrication of the flake powder samples.

The ball milling process was implemented using a mixer and mill device. It consisted of hardened steel vials, and the balls had a ball-to-powder weight ratio of 66:1. The milling process was performed in acetone for 12 h. As Gd has a high plasticity, the pieces of the ribbons for the treatments under consideration experienced only a plastic deformation during the first few hours. As the overall area of the cuttings increased, their thickness decreased. The change in the processing features took place after six hours of milling. The grinding process was accompanied by a decrease in the geometric dimensions of the pieces of ribbons. Special purposeful calibrations indicated that a milling time of about 10 h was sufficient for ensuring a steady-state Gd flake microstructure. Figure 1 shows the general view of the powder particles. It can be seen that they are flakes with an irregular shape, the size of which reach approximately 200 μm . Then the Gd powder samples were dried and annealed in glass, evacuated sealed tubes at temperatures of 350, 450, 500, 550 and 600 K for 30 min for each of the temperatures.

The structural investigation of the samples was performed by X-ray diffraction technique (XRD) using a Bruker D8 Advance diffractometer operating with Cu-K α radiation (wavelength $\lambda = 1.5406$ Å). The powder samples for the structural studies at room temperature were uniformly placed onto a zero-background silicon plate embedded in a generic sample holder.

A Quantum Design SQUID magnetometer (MPMS XL7) was used for the measurements of the magnetic properties of the samples. The magnetic entropy change $\Delta S_M(H, T)$ around the Curie temperature (T_C) was calculated on the basis of the Maxwell relation following the standard procedure described in ref [1].

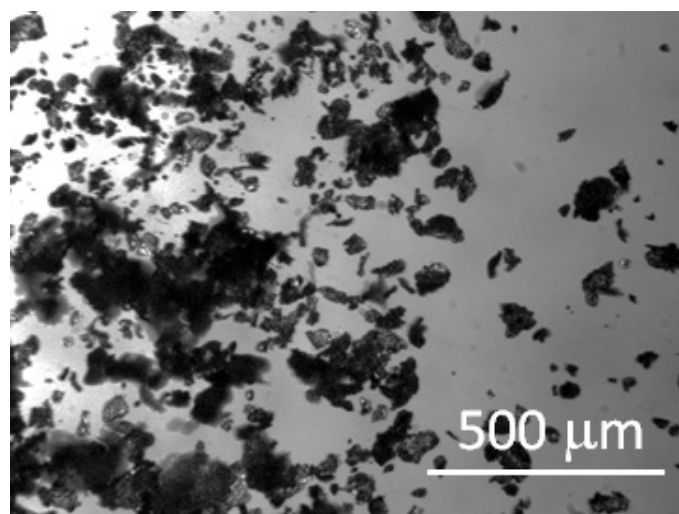


Figure 1. General view of the flake samples of Gd after 10 h of the milling process (optical microscopy).

3. Results and Discussion

According to X-ray studies, the main phase of the powder sample in the initial state (without heat treatments) was Gd with a hexagonal structure (Figure 2). In addition, the GdH_2 phase was present. It is known that for the formation of gadolinium hydride, extreme conditions are not required [25,26]. Here, the powders were ground in acetone, and the kinetic energy of the balls was sufficient to noticeably increase the local temperature on the surface of the particles. Therefore, the possibility of the formation of gadolinium hydride on the surface of Gd powder particles during grinding seems quite logical.

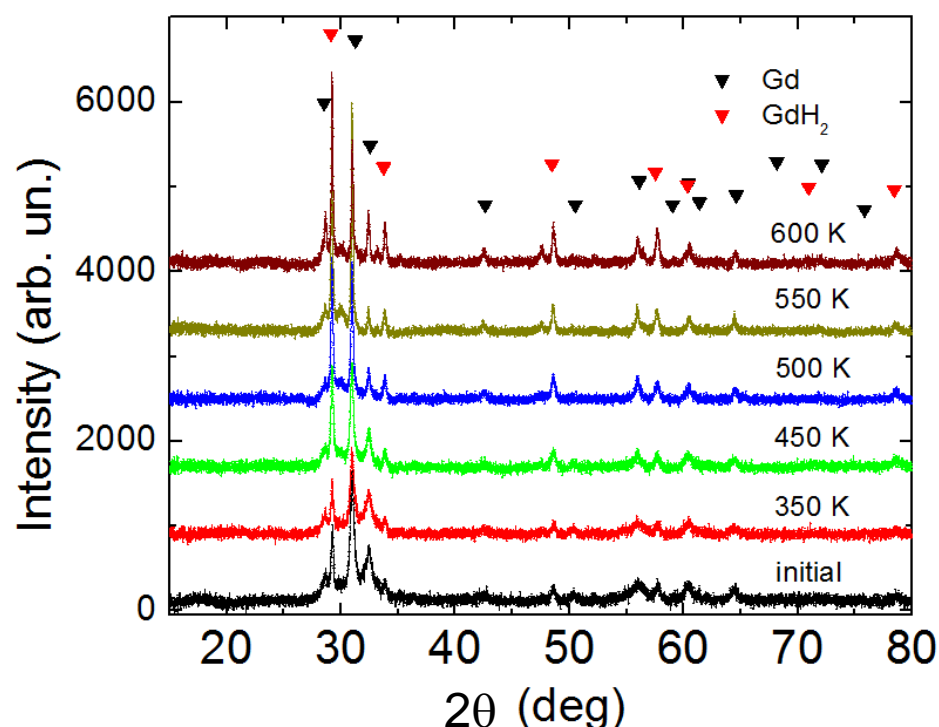


Figure 2. X-ray diffraction patterns of Gd powder samples in the initial state and after annealing at different temperatures. The reflexes corresponding to the hexagonal close-packed gadolinium Gd and GdH_2 phases are shown by different symbols, as indicated in the legend.

Its presence might play a positive protective role in preventing flakes from additional deep oxidation during heat treatments. Heat treatments help relieve stresses, reduce the number of vacancies and increase the average size of the grains. The grain size was calculated using the Scherrer formula for Gd hcp (002) reflection ($2\theta \approx 31.1^\circ$). For the Gd powder in the initial state, the average grain size was close to 30 ± 5 nm. An increase in the annealing temperature T_{ann} was accompanied by an increase in the grain size, especially at $T_{\text{ann}} > 450$ K (Figure 3). After annealing at 600 K, the average grain size was increased up to 150 ± 10 nm.

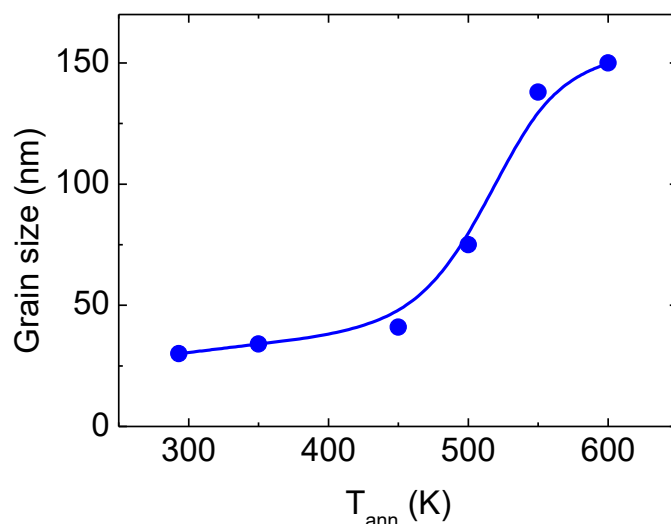


Figure 3. The average grain size depended on the annealing temperature. Data obtained from the XRD analysis.

Figure 4 shows the temperature dependence of magnetization $M(T)$ for Gd flake powder samples after the heat treatments at different temperatures. $M(T)$ curves were measured under the application of the magnetic field of 0.1 T in the field cooling regime. The position of the minimum of the dM/dT versus the temperature plot indicated that the Curie temperature T_C of the samples did not significantly change as a result of the heat treatments. The observed value of the Curie temperature was very close to the T_C value for polycrystalline bulk Gd, which is well-known from previous studies [1,20].

The so-called Arrott plots (M^2 versus H/M plots) derived from magnetization isotherms are useful for magnetocaloric properties analysis. Therefore, they were also obtained for all samples. As a typical example, Figure 5 shows M^2 vs H/M plots for Gd powders after heat treatments at 350, 500 and 600 K. For all mentioned samples, the Arrott plots exhibited a positive slope for the curves at all temperatures, indicating that a second-order magnetic transition from ferromagnetism to paramagnetism occurred around T_C , as prescribed by the Banerjee criterion [27]. From the Arrott plots, the Curie temperature was obtained in agreement with the value worked out with the minimum of the dM/dT versus the temperature plot method.

In addition, the shape of the experimental curves confirmed the assumption about a decrease in the defectiveness of the powders under the effect of annealing, made above, based on the analysis of the $M(T)$ dependences. It is known that the M^2 versus H/M plots are linear for homogeneous ferromagnetic materials [28]. The deviation from linearity suggests the presence of an inhomogeneous structure [29]. It can be seen that for the samples under consideration, the M^2 versus H/M plots linearity in the high field region improved for the powder annealed at 500 K (Figure 5).

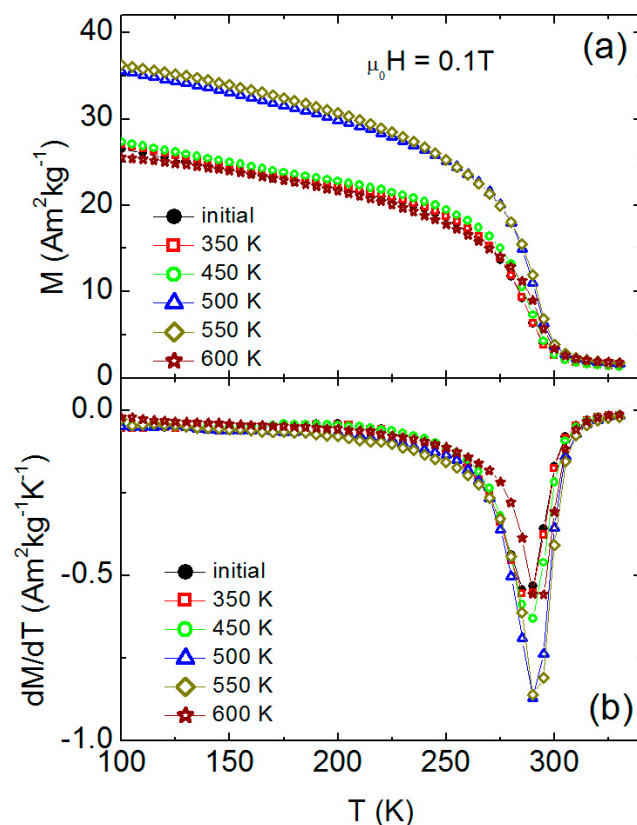


Figure 4. Temperature dependence of magnetization for Gd flake powders after the heat treatments at different temperatures (a); the corresponding plot of dM/dT versus temperature for the same heat treatments (b).

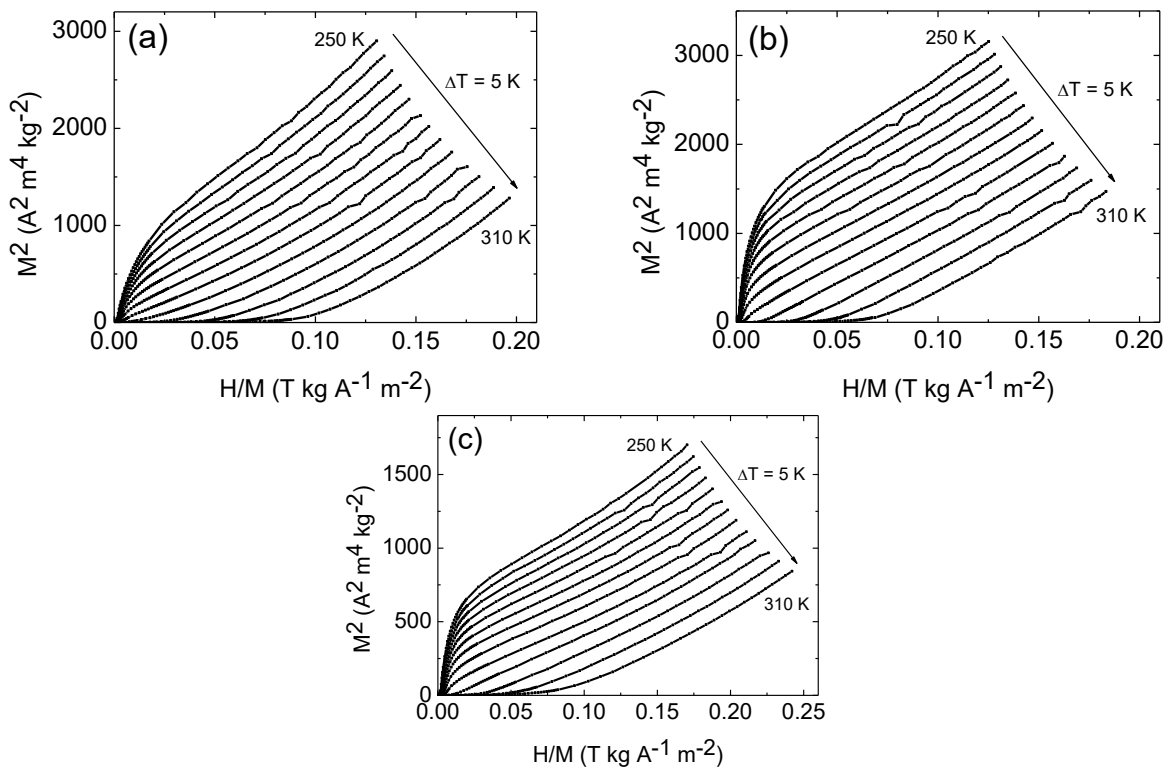


Figure 5. Arrott plots obtained for the Gd powder samples after heat treatments at 350 K (a), 500 K (b) and 600 K (c).

Figure 6 shows some of the measured experimental M–H curves analyzed for the magnetic entropy change calculations. The magnetization value of the flake powders was significantly smaller than the magnetization value of bulk gadolinium at low temperatures. It is worth mentioning that the magnetization of the gadolinium powder did not reach magnetic saturation even in the high external magnetic field of the order of 7 T.

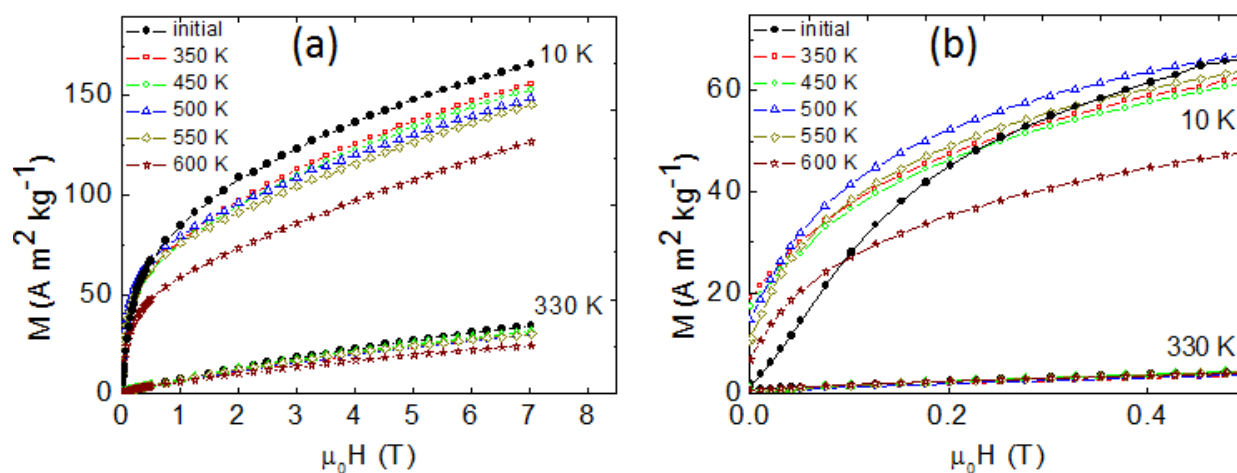


Figure 6. Magnetic field dependence of the magnetization M of the Gd flake powder samples measured at the temperatures of 10 and 330 K after previous heat treatments at different temperatures (as indicated in the legend) (a). The same behavior shown for the low field interval (b).

The observed behavior of the magnetization can be understood taking into account the results of the structural change, i.e., nanostructuring of Gd powder and the consequent change in the grain size. We considered that the ball milling process during a sufficiently long time could increase the dispersion of crystallite sizes, the relative volume fraction of the grain boundaries, the level of the stresses and the number of vacancies. Such changes can lead to a spin disorder in nanocrystalline gadolinium samples and, consequently, to a wide distribution of the Curie temperatures [30].

Figure 4 shows that after annealing at temperatures from 500 K to 550 K, the initial slope of the magnetization was steeper near the Curie temperature. This meant that the magnetic phase transition from the paramagnetic to ferromagnetic state in these kinds of samples occurred in a narrower temperature range. This may be due to the relaxation of lattice imperfections and the increase in the average grain size of the flakes.

Annealing at the temperature $T = 600$ K led to the degradation of the magnetic properties of the powder sample (Figure 4). Perhaps this was a consequence of the intensification of the Gd oxidation process by residual gases at such an elevated temperature. However, at 10 K, there was a region of the external magnetic fields (up to 0.5 T) for which the M value for the samples annealed at 500 K and showed the highest value.

In order to quantitatively describe the magnetic entropy change, the isothermal magnetization measurements were conducted in the external magnetic field up to its maximum value of 7 T in temperature from 10 to 330 K. Near the Curie temperature, the small step of 5 K was used. The standard Maxwell relation [1] was employed for the magnetic entropy ΔS_M change calculation through magnetic isotherms using the following equation:

$$\Delta S_M = \int_0^H \left(\frac{\partial M}{\partial T} \right)_H dH, \quad (1)$$

where H is the external magnetic field, M is magnetization and T is the temperature.

Figure 7 shows the magnetic entropy changes $\Delta S_M(T)$ for different values of $\Delta \mu_0 H$. The calculated ΔS_M magnitudes in the cases under consideration were smaller than the corresponding values for the bulk gadolinium samples previously reported [1,17].

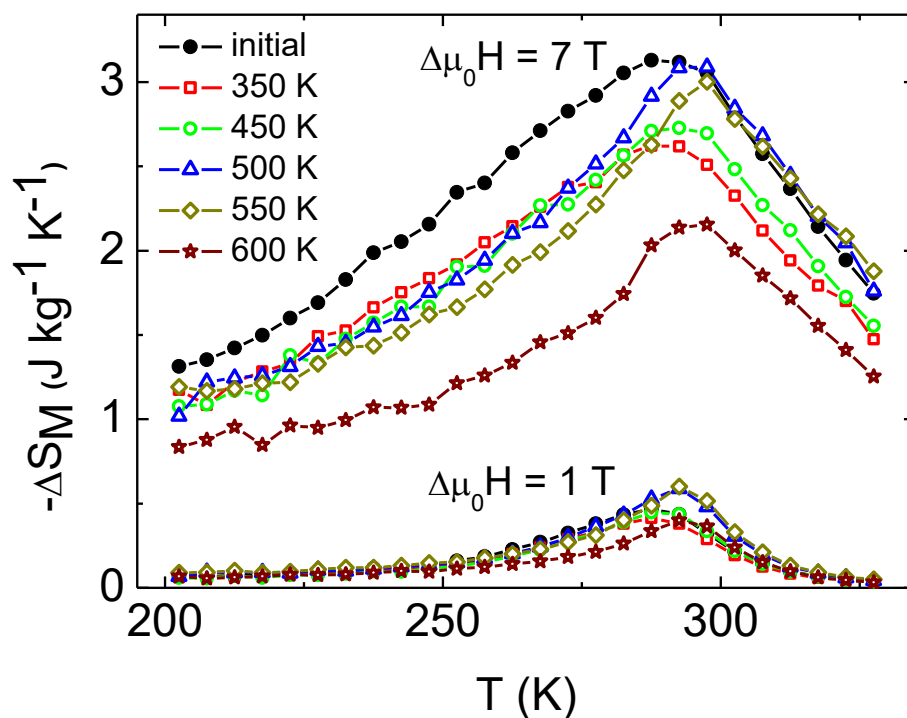


Figure 7. Temperature dependence of the magnetic entropy change at the values of the external magnetic field of 1 and 7 T for the Gd flake powder samples after the heat treatments at different temperatures.

The temperature at which the maximum of the $\Delta S_M(T)$ dependences appeared tended to increase with an increase in the annealing temperature. This result can be understood by taking into account the same reasons related to the structural peculiarities that were mentioned above when discussing the temperature dependence of magnetization. We, therefore, could explain the decrease in the value of the magnetic entropy changes $\Delta S_M(T)$ after annealing at $T = 600$ K as an expected consequence of a significant decrease in magnetization (Figure 6).

Although the isothermal magnetic entropy change was very important for the evaluation of the magnetocaloric properties, the refrigeration capacity should also be estimated and taken into account, as it is a very important technological parameter. The $\Delta S_M(T)$ curves for Gd powder samples have wider characteristic peaks, and the width of the ΔS_M peaks at its half-height is higher in comparison with data for the bulk Gd. Therefore, the value of the refrigerating capacity in the case of a Gd ball milled sample (Figure 8) was not significantly lower with respect to the refrigerating capacity value typical for the bulk gadolinium [1,23] or for microparticles of gadolinium of hundreds of microns size [6].

An important way to increase the efficiency of magnetic cooling is to increase the sensitivity of magnetocaloric materials with respect to the applied magnetic field [1,17]. For magnetocaloric materials characterized by the second-order phase transition, the power law can describe the dependence of the change in the magnetic entropy peak with respect to the applied magnetic field: $\Delta S_M^{\max} \propto H^n$. In the case of a single-phase material, the n value is expected to be $n = 2/3$ near T_C [1].

Figure 9 shows the change of ΔS_M^{\max} with respect to the magnetic field for the Gd powder samples after different temperatures of the heat treatment. Values of the exponent n are given in Table 1. It is seen that annealing at the selected conditions for the samples under consideration did not increase the n value.

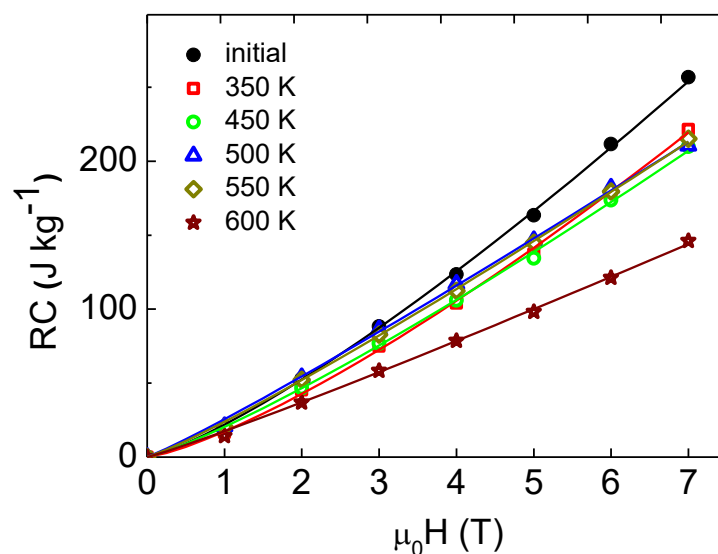


Figure 8. The refrigeration capacity as a function of the magnetic field for the Gd powder samples after the heat treatment at different temperatures.

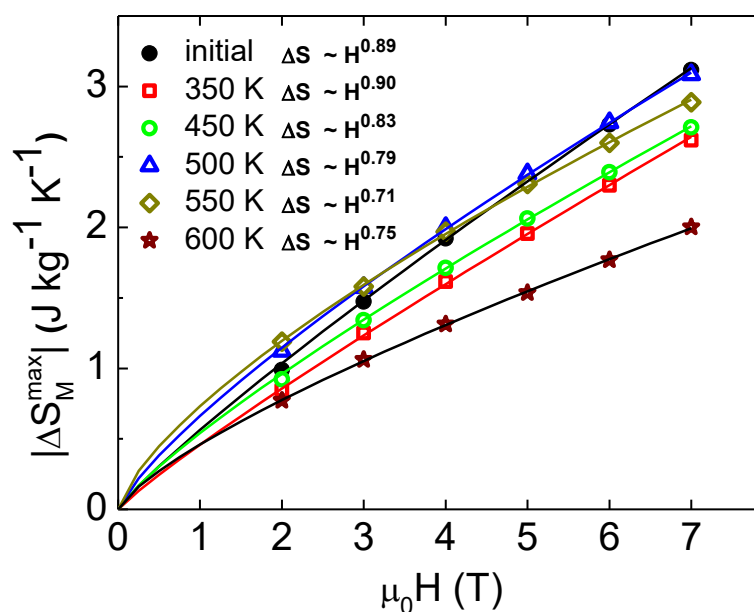


Figure 9. The maximum entropy changes as a function of magnetic field for the Gd powder samples after the heat treatment at different temperatures.

Table 1. Values of the ΔS_M^{\max} at $H = 1$ T and the exponent in the low power: $\Delta S_M^{\max} \propto H^n$ for the Gd powder samples after different temperatures of the heat treatment. Some data from the literature are also given for comparison.

Sample	Exponent n	ΔS_M^{\max} (J kg ⁻¹ K ⁻¹)
initial	0.89	0.5
350 K	0.90	0.4
450 K	0.83	0.5
500 K	0.79	0.6
550 K	0.71	0.6
600 K	0.75	0.4
Gd bulk	0.78 [14]	2.8 [1]

Although used in fabrication conditions, the heat treatment processes do not lead to an increase in the magnetocaloric effect, as was previously observed in the case of the bulk Gd samples [17]. Powder materials allow a much better heat transfer between the working refrigerating body and the surroundings simply due to the higher surface-to-volume ratio. As the technological steps for the fabrication of real devices may include different heat treatments, the obtained results could be useful for the estimation of their possible impact. In addition, the obtained materials should demonstrate high time stability as their surface is passivated, but the following problem should be additionally investigated.

4. Conclusions

Gd ribbons were obtained by a rapid quenching technique. They were used for the fabrication of Gd powders by a ball milling method. The structural features, magnetic and magnetocaloric properties of the produced powder materials were studied in an initial state and after heat treatments in a vacuum at temperatures of 350, 450, 500, 550 and 600 K for 40 min. It was shown that there was an annealing temperature range in which the relaxation of lattice imperfections and an increase in the average grain size occurred. This caused a narrowing of the temperature range in which the magnetic phase transitions of “ferro–para type” took place in such nanostructured samples.

Author Contributions: Conceptualization, A.V.S., D.S.N. and G.V.K.; methodology, D.S.N. and S.V.A.; software, A.V.A.; validation, D.S.N. and A.V.S.; formal analysis, G.V.K. and S.V.A.; investigation, D.S.N., N.V.S., A.L. and G.V.K.; data curation, G.V.K.; writing—original draft preparation, A.V.S. and G.V.K.; writing—review and editing, A.V.S., D.S.N. and G.V.K.; visualization, A.V.A., N.V.S. and A.L.; supervision A.V.S. All authors have discussed the results and implications and have commented on the manuscript at all stages. All authors have read and agreed to the published version of the manuscript.

Funding: The research funding from the Ministry of Science and Higher Education of the Russian Federation (Ural Federal University Program of Development within the Priority-2030 Program) is gratefully acknowledged. This research was supported in part by the Universidad del País Vasco/Euskal Herriko Unibertsitatea UPV/EHU Research Groups Funding.

Institutional Review Board Statement: This work did not involve humans or animals and therefore did not require an Institutional Review Board Statement and approval.

Informed Consent Statement: Not applicable.

Data Availability Statement: Data are available from the corresponding author upon reasonable request.

Conflicts of Interest: The authors declare no conflict of interest.

References

1. Franco, V.; Blázquez, J.S.; Ipus, J.J.; Law, J.Y.; Moreno-Ramírez, L.M.; Conde, A. Magnetocaloric effect: From materials research to refrigeration devices. *Prog. Mater. Sci.* **2018**, *93*, 112–232. [[CrossRef](#)]
2. Chzhan, V.B.; Kurganskaya, A.A.; Tereshina, I.S.; Karpenkov, A.Y.; Ovchenkova, I.A.; Tereshina-Chitrova, E.A.; Andreev, A.V.; Gorbunov, D.I.; Lushnikov, S.A.; Verbetsky, V.N. Influence of interstitial and substitutional atoms on magnetocaloric effects in RNi compounds. *Mater. Chem. Phys.* **2021**, *264*, 124455. [[CrossRef](#)]
3. Li, L.; Yan, M. Recent progress in the development of $RE_2TMTM'O_6$ double perovskite oxides for cryogenic magnetic refrigeration. *J. Mater. Sci. Technol.* **2023**, *136*, 1–12. [[CrossRef](#)]
4. Xu, P.; Hu, L.; Zhang, Z.; Wang, H.; Li, L. Electronic structure, magnetic properties and magnetocaloric performance in rare earths (RE) based RE_2BaZnO_5 (RE = Gd, Dy, Ho, and Er) compounds. *Acta Mater.* **2022**, *236*, 118114. [[CrossRef](#)]
5. Zhang, Y.; Li, S.; Hu, L.; Wang, X.; Li, L.; Yan, M. Excellent magnetocaloric performance in the carbide compounds $RE_2Cr_2C_3$ (RE = Er, Ho, and Dy) and their composites. *Mater. Today Phys.* **2022**, *27*, 100786. [[CrossRef](#)]
6. Gao, Q.; Yu, B.F.; Wang, C.F.; Zhang, B.; Yang, D.X.; Zhang, Y. Experimental investigation on refrigeration performance of a reciprocating active magnetic regenerator of room temperature magnetic refrigeration. *Int. J. Refrig.* **2006**, *29*, 1274–1285. [[CrossRef](#)]
7. Blázquez, J.S.; Ipus, J.J.; Moreno-Ramírez, L.M.; Borrego, J.M.; Lozano-Pérez, S.; Franco, V.; Conde, C.F.; Conde, A. Analysis of the magnetocaloric effect in powder samples obtained by ball milling. *Metall. Mater. Trans. E* **2015**, *2*, 131–138. [[CrossRef](#)]

8. Chrobak, A.; Bajorek, A.; Chełkowska, G.; Haneczok, G.; Kwiecień, M. Magnetic properties and magnetocaloric effect of $\text{Gd}(\text{Ni}_{1-x}\text{Fex})_3$ crystalline compound and powder. *Phys. Status Solidi A* **2009**, *206*, 731–737. [[CrossRef](#)]
9. Iglesias-Rey, R.; Vieites-Prado, A.; Argibay, B.; Campos, F.; Bañobre-López, M.; Sobrino, T.; Rivas, J.; Castillo, J. Magnetocaloric effect for inducing hypothermia as new therapeutic strategy for stroke: A physical approach. *J. Appl. Biomed.* **2017**, *15*, 33–38. [[CrossRef](#)]
10. Pires, A.L.; Belo, J.H.; Turcaud, J.; Oliveira, G.N.P.; Araújo, J.P.; Berenov, A.; Cohen, L.F.; Lopes, A.M.L.; Pereira, A.M. Influence of short time milling in $\text{R}_5(\text{Si,Ge})_4$, R = Gd and Tb, magnetocaloric materials. *Mater. Des.* **2015**, *85*, 32–38. [[CrossRef](#)]
11. Svalov, A.V.; Arkhipov, A.V.; Andreev, S.V.; Neznakhin, D.S.; Larrañaga, A.; Kurlyandskaya, G.V. Modified field dependence of the magnetocaloric effect in Gd powder obtained by ball milling. *Mater. Lett.* **2021**, *284*, 128921. [[CrossRef](#)]
12. Kurlyandskaya, G.V.; Safronov, A.P.; Bhagat, S.M.; Lofland, S.E.; Beketov, I.V.; Marcano Prieto, L. Tailoring functional properties of Ni nanoparticles-acrylic copolymer composites with different concentrations of magnetic filler. *J. Appl. Phys.* **2015**, *117*, 123917. [[CrossRef](#)]
13. Sedoi, V.S.; Ivanov, Y.F. Particles and crystallites under electrical explosion of wires. *Nanotechnology* **2008**, *19*, 145710. [[CrossRef](#)] [[PubMed](#)]
14. Blázquez, J.S.; Ipus, J.J.; Moreno-Ramírez, L.M.; Álvarez-Gómez, J.M.; Sánchez-Jiménez, D.; Lozano-Pérez, S.; Franco, V.; Conde, A. Ball milling as a way to produce magnetic and magnetocaloric materials: A review. *J. Mater. Sci.* **2017**, *52*, 11834–11850. [[CrossRef](#)]
15. Hirian, R.; Souca, G.; Popa, F.; Gutoiu, S.; Pop, V.; Isnard, O.; Tetean, R. Interphase exchange coupling and magnetocaloric effect in $\text{Co}_3\text{Gd}_4/\text{Co}_7\text{Gd}_{12}$ magnetic nanocomposites, obtained by mechanical milling. *J. Magn. Magn. Mater.* **2022**, *559*, 169505. [[CrossRef](#)]
16. Starostenko, S.N.; Petrov, D.A.; Rozanov, K.N.; Shiryaev, A.O.; Lomaeva, S.F. Effect of temperature on microwave permeability of an air-stable composite filled with gadolinium powder. *Sensors* **2022**, *22*, 3005. [[CrossRef](#)]
17. Doblas, D.; Moreno-Ramírez, L.M.; Franco, V.; Conde, A.; Svalov, A.V.; Kurlyandskaya, G.V. Nanostructuring as a procedure to control the field dependence of the magnetocaloric effect. *Mater. Des.* **2017**, *114*, 214–219. [[CrossRef](#)]
18. Moreno-Ramírez, L.M.; Law, J.Y.; Pramana, S.S.; Giri, A.K.; Franco, V. Analysis of the magnetic field dependence of the isothermal entropy change of inverse magnetocaloric materials. *Results Phys.* **2021**, *22*, 103933. [[CrossRef](#)]
19. Burkhanov, G.S.; Kolchugina, N.B.; Tereshina, E.A.; Tereshina, I.S.; Politova, G.A.; Chzhan, V.B.; Badurski, D.; Chistyakov, O.D.; Paukov, M.; Drulis, H.; et al. Magnetocaloric properties of distilled gadolinium: Effects of structural inhomogeneity and hydrogen impurity. *Appl. Phys. Lett.* **2014**, *104*, 242402. [[CrossRef](#)]
20. Gottschall, T.; Kuz'min, M.D.; Skokov, K.P.; Skourski, Y.; Fries, M.; Gutfleisch, O.; Ghorbani Zavareh, M.; Schlagel, D.L.; Mudryk, Y.; Pecharsky, V.; et al. Magnetocaloric effect of gadolinium in high magnetic fields. *Phys. Rev. B* **2019**, *99*, 134429. [[CrossRef](#)]
21. Kuz'min, M.D. Shape of temperature dependence of spontaneous magnetization of ferromagnets: Quantitative analysis. *Phys. Rev. Lett.* **2005**, *94*, 107204. [[CrossRef](#)] [[PubMed](#)]
22. Kuz'min, M.D.; Skokov, K.P.; Diop, L.V.B.; Radulov, I.A.; Gutfleisch, O. Exchange stiffness of ferromagnets. *Eur. Phys. J. Plus* **2020**, *135*, 301. [[CrossRef](#)]
23. Taskaev, S.V.; Buchelnikov, V.D.; Pellenen, A.P.; Kuz'min, M.D.; Skokov, K.P.; Karpenkov, D.Y.; Bataev, D.S.; Gutfleisch, O. Influence of thermal treatment on magnetocaloric properties of Gd cold rolled ribbons. *J. Appl. Phys.* **2013**, *113*, 17A933. [[CrossRef](#)]
24. Svalov, A.; Andreev, S.; Arkhipov, A.; Kudyukov, E.; Neznakhin, D.; Larrañaga, A.; Kurlyandskaya, G. Magnetic and magnetocaloric properties of Gd melt-spun ribbons. *J. Phys. Conf. Ser.* **2019**, *1389*, 012100. [[CrossRef](#)]
25. Hémon, S.; Cowley, R.A.; Ward, R.C.C.; Wells, M.R.; Douysset, L.; Ronnow, H. Magnetic structure of Gd, GdH_2 and NdH_2 single crystal films. *J. Phys. Condens. Matter.* **2000**, *12*, 5011–5020. [[CrossRef](#)]
26. Tessier, P.; Fruchart, D.; Givord, D. Magnetic properties of epitaxial gadolinium hydride films. *J. Alloys Compd.* **2002**, *330*, 369–372. [[CrossRef](#)]
27. Banerjee, S.K. On a generalised approach to first and second order magnetic transitions. *Phys. Lett.* **1964**, *12*, 16–17. [[CrossRef](#)]
28. Herzer, G.; Fähnle, M.; Egami, T.; Kronmüller, H. Micromagnetic theory of phase transitions in inhomogeneous ferromagnets III. Non-local Landau-Ginzburg theory. *Phys. Stat. Sol. B* **1980**, *101*, 713–721. [[CrossRef](#)]
29. Nair, H.S.; Swain, D.; Adiga, S.; Hariharan, N.; Narayana, C.; Elizabeth, S. Griffiths phase-like behavior and spin-phonon coupling in double perovskite $\text{Tb}_2\text{NiMnO}_6$. *J. Appl. Phys.* **2011**, *110*, 123919. [[CrossRef](#)]
30. Döbrich, F.; Kohlbrecher, J.; Sharp, M.; Eckerlebe, H.; Birringer, R.; Michels, A. Neutron scattering study of the magnetic microstructure of nanocrystalline gadolinium. *Phys. Rev. B* **2012**, *85*, 094411. [[CrossRef](#)]